

Cite this: *Sustainable Food Technol.*,  
2023, 1, 426

# Encapsulation of essential oils using hemp protein isolate–gum Arabic complex coacervates and evaluation of the capsules

Xinye Liu,<sup>a</sup> Feng Xue<sup>ID</sup>\*<sup>b</sup> and Benu Adhikari<sup>ID</sup>\*<sup>ac</sup>

Complex coacervates between hemp protein isolate and gum Arabic were prepared and used as an emulsifier and encapsulant for four different essential oils (oregano, mustard, grapefruit and lemon). The properties of the capsules including encapsulation efficiency, ability to disperse in the aqueous phase, thermal stability, microstructure, release pattern, and antioxidative and antibacterial properties were determined and found to be affected by the type or nature of the essential oil used. The capsules of oregano essential oil showed the highest encapsulation efficiency, ability to disperse in the aqueous phase, most compact structure, highest thermal stability, antioxidant activity and the slowest release rate. Capsules of each essential oil had better antibacterial activity than their corresponding free/unencapsulated state, except for oregano essential oil in which the free essential oil exhibited higher antibacterial activity than the corresponding capsules. The release of essential oil from each capsule was fitted well using the Weibull model and showed a complex release mechanism including matrix erosion. This study contributes to the science and technology to deliver essential oil microcapsules through a benign (complex coacervation) pathway and contributes sustainability by offering an alternative pathway to utilize hemp protein (which is still a by-product of the hemp oil industry).

Received 9th January 2023  
Accepted 27th March 2023DOI: 10.1039/d3fb00004d  
rsc.li/susfoodtech

## Introduction

Essential oils are natural aromatic and volatile compounds extracted from flowers, leaves, seeds, roots, buds and stems of plants.<sup>1</sup> They contain many bioactive compounds such as tertiary terpene alcohols, aliphatic terpene ethers, aromatic terpene hydrocarbons and phenolic and flavonoid compounds.<sup>2</sup> Therefore, essential oils are considered to possess many functional properties, such as antioxidative,<sup>3</sup> antimicrobial<sup>4</sup> and anti-inflammatory.<sup>5</sup> However, they are highly volatile, sensitive to environmental conditions (such as oxygen, temperature and light) during storage and have low water solubility, all of which have limited their greater application in the food industry.

Encapsulation is a viable method which enables entrapment and retaining of bioactive compounds within the shell/wall matrix to enhance their solubility in water and improve physicochemical stability against adverse environmental conditions.<sup>6</sup> Thus, encapsulation technologies are widely used to facilitate the controlled release of essential oils as well as improve their stability and water solubility.<sup>7</sup> The wall materials play an important role in the encapsulation of essential oils; thus, they

should have excellent emulsifying properties as well as good ability to disperse in the aqueous phase.

Protein–polysaccharide complexes could meet the above-mentioned requirements as they combine the characteristics of proteins to adsorb strongly at the oil–water interface with the solubility of polysaccharides in the aqueous phase. The protein–polysaccharide complexes can be obtained by covalent conjugation and non-covalent complexation. The Maillard reaction has been widely used to achieve covalent bonding (covalent conjugation) between proteins and polysaccharides, and the resulting conjugates have been applied to encapsulate essential oils.<sup>8,9</sup> However, the Maillard reaction usually requires elevated temperature (60–70 °C for the dry-heating route and 70–100 °C for the wet-heating route) and a long reaction time (1–14 days for the dry-heating route and 5–24 h for wet-heating route) to induce the reaction. The elevated temperature and long exposure time impart products with an undesirable brown colour.<sup>10,11</sup> Furthermore, the dry-heating process cannot be easily scaled up to an industrial scale and the critical precise control of relative humidity on the headspace is difficult.<sup>12,13</sup> The wet-heating route has been applied to the industrial scale; however, time–temperature combination is quite difficult in order to control the formation of advanced glycation end products (AGEs) which should be strictly avoided.<sup>14</sup> Non-covalent complexation makes use of electrostatic interaction to induce complex coacervation between the protein and polysaccharide. Complex coacervates are also widely used to

<sup>a</sup>School of Science, RMIT University, Melbourne, VIC 3083, Australia<sup>b</sup>School of Pharmacy, Nanjing University of Chinese Medicine, Nanjing 210023, China. E-mail: xuefeng@njucm.edu.cn; Tel: +86 13805194382<sup>c</sup>Centre for Advanced Materials and Industrial Chemistry (CAMIC), Melbourne, VIC 3001, Australia. E-mail: benu.adhikari@rmit.edu.au; Tel: +61 3 99259940

encapsulate essential oils and shown to enhance their stability and sustained release.<sup>15–17</sup>

Gum Arabic has been the polysaccharide of choice to prepare complex coacervates with a wider range of proteins (pea proteins,<sup>18</sup> gelatin,<sup>19</sup> rice glutelin,<sup>20</sup> whey proteins<sup>21</sup> and soy proteins<sup>22</sup>) due to its excellent emulsifying properties, solubility in the aqueous phase and possession of negative charge for most of the pH range. Gum Arabic–protein complex coacervates are known to possess excellent ability to encapsulate bioactive compounds. Hence, it is of practical importance to further investigate how new proteins (*e.g.*, hemp protein) undergo complex coacervation with gum Arabic and how the resulting complex coacervates perform as encapsulating shell materials.

So far, hemp protein is a by-product of the hemp oil industry. However, it is attracting greater attention as an alternative protein. Hemp protein also contains a high amount of arginine, glutamic acid, and sulfur-containing amino acids.<sup>23</sup> Thus, its alternative application will minimize the waste stream of the hemp oil industry and contribute to sustainability. Recently, the complex coacervation process between hemp protein and a number of common food gums was studied with a specific focus on the optimization of the process and characterization of the resulting complex coacervates.<sup>24</sup> In particular hemp protein–gum Arabic complex coacervates were suggested to be useful wall materials for encapsulation of bioactive compounds.<sup>25</sup> However, the effectiveness of hemp protein–gum Arabic complex coacervates as an emulsifier and wall material to emulsify and encapsulate the essential oil is not studied.

Therefore, this study aimed at investigating how effectively commonly available essential oils (oregano, lemon, mustard and grapefruit) could be emulsified and encapsulated in hemp protein isolate (HPI)–gum Arabic (GA) complex coacervates. The physicochemical properties, release pattern, and antioxidative and antimicrobial properties of the capsules of each of the four essential oils produced using HPI–GA complex coacervates were evaluated.

## Materials and methods

### Materials and chemicals

The hemp seed (*Cannabis sativa* L.) sample was purchased from Yunnan Industrial Hemp Co., Ltd (Kunming, Yunnan, China). The seeds were ground with a coffee grinder (Breville, BCG300, Australia) and sieved through to obtain a size fraction below 250  $\mu\text{m}$ . This ground powder was used for protein extraction. Four essential oils (Mustard, lemon, grapefruit and oregano essential oils) were purchased from Shanghai Yuanye Bio-Technology Co., Ltd (Shanghai, China). The 1,1-diphenylpicryl phenyl hydrazine (DPPH) free radical and 2,2'-azino-bis (3-ethylbenzothiazoline-6-sulfonic acid) ammonium salt (ABTS) free radical were purchased from Shanghai Yuanye Bio-Technology Co., Ltd (Shanghai, China). The strains of *Escherichia coli* (CMCC 44102) and *Bacillus subtilis* (CMCC 63501) were also purchased from the same company. Gum Arabic, KBr and ethanol were purchased from Sinopharm Chemical Reagent Co., Ltd (Shanghai, China). All the reagents used in this study were of analytical grade and were used as received.

### Extraction of hemp protein isolate

Hemp protein isolate (HPI) was extracted according to our previous study.<sup>26</sup> Briefly, the oil was first extracted from the ground hemp seed powder in *n*-hexane. The defatted meal was used to extract protein following an alkaline extraction protocol for which MilliQ water was used at pH 10.0 as the extracting medium. The protein component was precipitated by adjusting the pH to 4.3 (isoelectric point) and the precipitate was collected by centrifugation at 2950 $\times g$  for 20 min. The collected protein mass was neutralized and freeze-dried ( $-50\text{ }^{\circ}\text{C}$  and 15 Pa for 48 h). The extraction yield of HPI ranged between 24.1 and 25.2% (based on the hemp meal weight). The protein content of the extracted HPI was determined to be  $90.5 \pm 1.6\%$  by using the Kjeldahl method (Unit-FOSS, Kjeltac 8200, Denmark) applying a conversion factor of 6.25.

### Preparation of HPI–gum Arabic complex coacervates

The HPI and gum Arabic (GA) mixed solutions were prepared with MilliQ water at room temperature at 1% wt solids. The ratio of HPI to GA was maintained at 4:1 and the pH of the mixed solution was adjusted to 3.5 using 1 M HCl to induce complex coacervation. The optimum HPI-to-gum Arabic ratio and pH values were obtained as per our previous study.<sup>24</sup> When the sufficient formation of complex coacervates was identified through the turbidity test, the aqueous slurry was centrifuged at 2950 $\times g$  for 30 min at room temperature to collect complex coacervates. The wet complex coacervate mass was freeze-dried as described in the preceding section.

### Encapsulation of essential oils by using HPI–GA complex coacervates

1 g of dry complex coacervate mass was dispersed in 100 mL Milli-Q water and then 1 g essential oil was added to the dispersion. A coarse emulsion was obtained by using a homogenizer (KINEMATICA, PT-MR 2100, Switzerland) operating at 10 000 rpm for 3 min. The coarse emulsion was further homogenized using an ultrasound device (0.636 cm titanium probe, NingBo Scientz Biotechnology Co. Ltd, Ningbo, China) at 400 W for 12 min in an ice-water bath.<sup>26</sup> The emulsion was freeze-dried for 48 h, and the dried sample was ground to obtain a free-flowing powder.

### Determination of encapsulation efficiency

The encapsulation efficiency (EE) of the freeze-dried microcapsules was determined using eqn (1). The surface oil was determined gravimetrically according to a previous study.<sup>27</sup> Briefly, a 2 g capsule mass was dispersed in 40 mL *n*-hexane with constant stirring (150 rpm) for 1 min. The extracted oil phase together with *n*-hexane was filtered and then centrifuged at 2950 $\times g$  at 4  $^{\circ}\text{C}$  for 10 min. The oil phase was collected after evaporation of *n*-hexane by using a rotary evaporator (40  $^{\circ}\text{C}$ ). The total oil was determined gravimetrically according to a previous study.<sup>28</sup> Briefly, a 2 g capsule mass was dispersed first in 12 mL of 4 N HCl. After total dissolution, 50 mL *n*-hexane was added to extract the oil. Then, the sample was centrifuged at



2950×g at 4 °C for 10 min and the oil phase together with *n*-hexane was recovered. The oil was obtained after evaporation of *n*-hexane.

$$EE (\%) = \frac{\text{Total oil (g)} - \text{Surface oil (g)}}{\text{Total oil (g)}} \times 100 \quad (1)$$

### Microstructure and particle size of capsules in dispersion

The capsules were dispersed in MilliQ water and the microstructure was observed by using a microscope (CMS, Leica Microsystems, Wetzlar, Germany). The volume-mean particle size was measured by using a laser diffraction particle size analyzer (Beckman Coulter Inc., LS 13320, USA) using distilled water as the dispersant. The refractive indices of 1.33 and 1.50 were used for dispersant and particles, respectively.

### Acquiring the Fourier transform infrared (FTIR) spectrum of capsules

The dry microcapsule sample was mixed with pure KBr and ground together and placed in a mould and then pressed into a transparent sheet using a hydraulic press. FTIR analysis was performed using an infrared spectrometer (Thermo Scientific Nicolet iS5, America) in the wavenumber range of 4000–400 cm<sup>-1</sup>. The sample was scanned for 32 times and averaged. Pure KBr was scanned to subtract the background.

### Thermal properties of capsules

In order to obtain mass loss *versus* temperature data, the sample (5 mg) was sealed in a ceramic pan and heated from 25 to 500 °C at a heating rate of 10 °C min<sup>-1</sup> using a thermogravimetric analyzer (Q500, TA Instruments, USA). To determine the pattern (endothermic and exothermic) of heat flow, the sample (5 mg) was sealed in an aluminum pan and heated at a rate of 10 °C min<sup>-1</sup> from 25 to 250 °C using a differential scanning calorimeter (TA Instruments, USA).

### Acquiring the microstructure of capsules

The microstructure of capsules was acquired by using a scanning electron microscope (SU8000, Japan) at an accelerating potential of 20 kV. The capsules were adhered to a conductive adhesive and coated with a thin layer of gold. The surface morphology of capsules was observed at a 10 000× magnification.

### Controlled release of essential oil from capsules

The controlled release of essential oil from capsules was determined according to a previous study.<sup>29</sup> A mixture of ethanol and water (ethanol : water = 50 : 50, v/v) was used as the simulant. Then, a 200 mg sample was placed inside dialysis bags (12 000 Da) and submerged in 50 mL of simulant. The calibration curve was obtained by diluting the individual essential oils with the release solvent and the absorbance was measured by using a spectrophotometer (Spark 10M, Tecan,

Switzerland, 96-well plates) at a wavelength of 274 nm. Release data were fitted to the Weibull model according to eqn (2).<sup>30</sup>

$$\ln(1 - Q) = -at^b \quad (2)$$

where *Q* is defined as the fraction of essential oil released from capsules, *a* is the proportionality constant and *b* (dimensionless) indicates the release mechanism.

### Measurement of antioxidant and antimicrobial properties

The antioxidant properties were measured according to previous studies.<sup>31,32</sup> In brief, the sample was mixed with DPPH (0.10 mM) or ABTS (7 mM) to obtain a final concentration of DPPH or ABTS in the range of 2.0 mg mL<sup>-1</sup>. After incubation for 30 min in the dark, the absorbance of the 200 μL sample was measured using a spectrophotometer (96-well plates, DPPH: 517 nm, ABTS: 734 nm).

Antibacterial activity was determined according to a previous study with minor modifications.<sup>33</sup> Luria–Bertani medium (25 mL) was poured into Petri dishes, which were previously seeded with 0.1 mL of inoculum containing about 10<sup>6</sup> CFU mL<sup>-1</sup> cells of indicator bacterium (*Escherichia coli* or *Bacillus subtilis*). The essential oil and its microcapsules were dissolved in 1% Tween-80 and diluted to 20 mg mL<sup>-1</sup> and was used in these tests. A sterilised piece of filter paper (10 mm diameter) that was loaded with 100 μL sample solution was placed on the plate and then incubated at 37 °C for 24 h. The diameter of the inhibition zone surrounding the sterilised filter paper was measured and recorded. The sterilised pieces of filter paper loaded with chloromycetin (positive control, 20 mg mL<sup>-1</sup>) and free essential oil samples (20 mg mL<sup>-1</sup>) were used to compare the antimicrobial properties of the capsules.

### Statistical analysis

All experiments were carried out in triplicate in terms of sample preparation and tests unless otherwise specified. The results are expressed as mean ± standard deviation. The data sets were analysed using SPSS25.0 (analysis software, Tallahassee, FL, USA). Analysis of Variance (ANOVA) was performed through a fully randomized linear modelling process. Significance difference was determined at a 95% confidence level (*p* < 0.05).

## Results and discussion

### Effect of essential oil type on the encapsulation efficiency

Published literature indicates that the encapsulation efficiency of essential oils in a complex coacervate matrix ranges from 32% to 96%, depending on the nature of the complex coacervates, core/wall ratio and drying method used.<sup>16,17,34,35</sup> As shown in Fig. 1 the encapsulation efficiency was in the range of 34–57% depending on the type of essential oil used. This result indicated that the encapsulation efficiency was significantly affected by the type or nature of essential oil. This could be due to varying degrees of interaction between compounds present in each essential oil and the complex coacervates. It was shown earlier that if the essential oil contained a proportionally higher



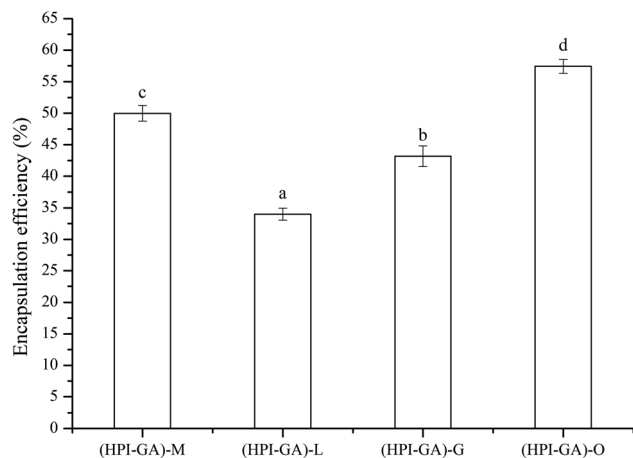


**Fig. 1** Encapsulation efficiency of essential oils encapsulated in hemp protein isolate (HPI)–gum Arabic (GA) complex coacervates. (HPI–GA): HPI–GA complex coacervate; (HPI–GA)–M: capsules of mustard (M) essential oil in (HPI–GA) complex coacervates; (HPI–GA)–L: capsules of lemon (L) essential oil in (HPI–GA) complex coacervates; (HPI–GA)–G: capsules of grapefruit (G) essential oil in (HPI–GA) complex coacervates; (HPI–GA)–O: capsules of oregano (O) essential oil in (HPI–GA) complex coacervates. Different letters mean values showed significant differences ( $p < 0.05$ ).

amount of small molecular hydrophilic compounds, the encapsulation efficiency could be improved as they act as surfactants.<sup>36</sup> If the essential oil contained a greater proportion of polyphenols, the adsorption layer (at the oil–water interface) could be disturbed due to the interaction between polyphenols and complex cocreates.<sup>37</sup> The breakdown or perturbation of the adsorption layer could lead to a phase separation and then decreases the encapsulation efficiency. The ability of fatty acids of essential oils to attach to and interact with the complex coacervate shell could also affect the encapsulation efficiency. A previous study showed that the fatty acids with longer chains could help polymers to better interact with the oil more effectively than those with shorter chains and then improve the stability of the emulsion.<sup>38</sup> Therefore, the encapsulation efficiency of essential oils in a complex coacervate matrix is highly dependent on their components. The main components (%) of mustard,<sup>39</sup> lemon,<sup>40</sup> grapefruit<sup>41</sup> and oregano<sup>42</sup> essential oils are summarised in Table 1. Isothiocyanate is the major component of mustard essential oil. Lemon and grapefruit essential oils possess a higher amount of limonene. Carvacrol is the major

component of oregano essential oil. The capsules loaded with oregano essential oil showed much higher (57%) encapsulation efficiency. This could be attributed to the fact that carvacrol contains a hydroxyl group and benzene ring, which could act as surfactants to improve the interfacial properties of coacervates. The capsules loaded with lemon essential oil showed much lower (34%) encapsulation efficiency, which could be attributed to the nonpolar feature of limonene. The capsules loaded with grapefruit essential oil also showed higher encapsulation efficiency than the ones containing lemon essential oil. This is probably due to the fact that grapefruit essential oil contained both limonene and carvacrol.

### Effect of essential oils on the microstructure of capsules in aqueous medium

The type or nature of essential oil significantly affected the dispersion of capsules in distilled water (Fig. 2). The capsules containing oregano essential oil were dispersed uniformly to a greater degree in the aqueous phase. This could be attributed to the excellent emulsifying properties of HPI–GA complex coacervates which can form an adsorption layer around the essential oil droplet, making it easier to distribute in the aqueous phase. However, the formation of aggregates was observed in capsules containing the other three essential oils. The degree of aggregation was highest in capsules containing lemon essential oil. The presence of aggregates could be attributed to the lower encapsulation efficiency of these oils which indicated that a higher amount of essential oil covered the surface of capsules which promoted the aggregation of encapsules through hydrophobic interaction. This observation was further supported by the fact that capsules had more extra free lemon and grapefruit essential oil droplets on their surface (as marked by a red circle in Fig. 2). This result also suggested that the major component (such as limonene) of lemon and grapefruit essential oils would not be easily emulsified/encapsulated by complex coacervates.

### Effect of essential oils on the particle size of capsules in the aqueous phase

The results of particle size are presented in Fig. 3. The particle size data were in accordance with the observation made on the microstructure in the preceding section. The capsules loaded with mustard and oregano essential oils exhibited monomodal size distribution, suggesting their better ability to disperse in

**Table 1** Main components (%) of essential oils [39–42]. EO = essential oil

Mustard EO	Lemon EO	Grapefruit EO	Oregano EO
2-Methylbutyronitrile (0.42%)	$\alpha$ -Pinene (1.14%)	3-Carene (6.31%)	Myrcene (1.50%)
3-Pentenitrile (1.14%)	$\beta$ -Pinene (5.43%)	Linalyl alcohol (14.13%)	$\alpha$ -Terpinene (1.66%)
Hexanal (0.30%)	Limonene (70.99%)	Limonene (23.77%)	$\gamma$ -Terpinene (5.20%)
Furfural (3.36%)	<i>o</i> -Cymene (3.30%)	$\alpha$ -Terpineol (14.36%)	<i>p</i> -Cymene (6.06%)
Isothiocyanate (86.33%)	Limonene (4.92%)	Carvacrol (17.42%)	$\beta$ -Caryophyllene (2.17%)
Benzene acetaldehyde (0.51%)	Verbenol (1.16%)	<i>D</i> -Carvone (10.88%)	Terpinen-4-ol (0.52%)
3-(Methylthio)propyl cyanide (0.86%)	Cyclohexen-1-ol (1.38%)	Benzyl cinnamate (5.02%)	Thymol (1.38%)
2-Phenylethyl cyanide (4.18%)	Carvacrol (3.74%)	Perillyl alcohol (2.96%)	Carvacrol (80.03%)





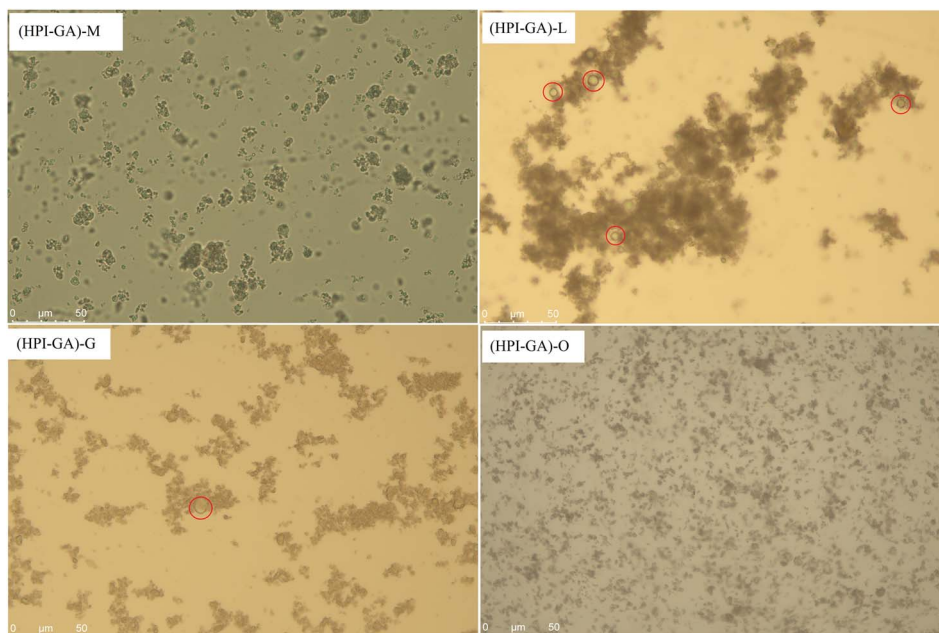


**Fig. 2** Microstructure of essential oils encapsulated in hemp protein isolate (HPI)–gum Arabic (GA) complex coacervates. (HPI–GA): HPI–GA complex coacervate; (HPI–GA)–M: capsules of mustard (M) essential oil in (HPI–GA) complex coacervates; (HPI–GA)–L: capsules of lemon (L) essential oil in (HPI–GA) complex coacervates; (HPI–GA)–G: capsules of grapefruit (G) essential oil in (HPI–GA) complex coacervates; (HPI–GA)–O: capsules of oregano (O) essential oil in (HPI–GA) complex coacervates.

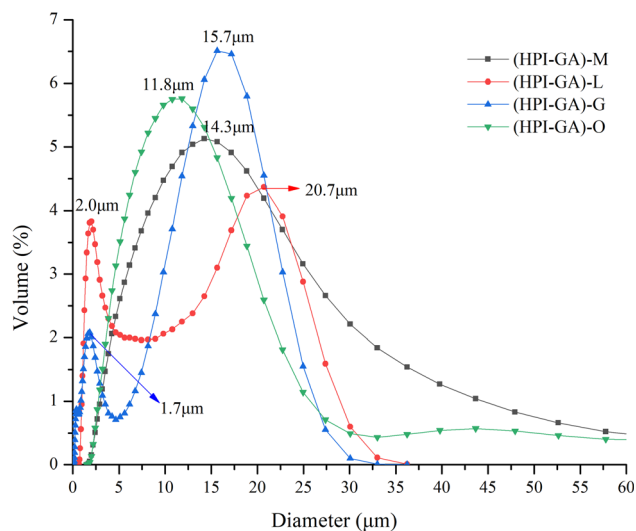


**Fig. 3** Particle size distribution of essential oils encapsulated in hemp protein isolate (HPI)–gum Arabic (GA) complex coacervates. (HPI–GA): HPI–GA complex coacervates; (HPI–GA)–M: capsules of mustard (M) essential oil in (HPI–GA) complex coacervates; (HPI–GA)–L: capsules of lemon (L) essential oil in (HPI–GA) complex coacervates; (HPI–GA)–G: capsules of grapefruit (G) essential oil in (HPI–GA) complex coacervates; (HPI–GA)–O: capsules of oregano (O) essential oil in (HPI–GA) complex coacervates.

the aqueous phase. However, the capsules loaded with lemon and grapefruit essential oils showed bimodal distribution in which the peak appearing at a higher size could be attributed to the aggregates and the peak appearing at a lower size could be

attributed to non-aggregated complex coacervates. In addition, the capsules loaded with oregano essential oil had much lower sizes, which further confirmed that the interaction between major components (*i.e.*, carvacrol) of oregano essential oil and complex coacervates was stronger than others. A previous study also reported that increased binding force between carvacrol and core/wall materials decreased the droplet size.<sup>43</sup>

#### Interaction of essential oils with the shell/wall of capsules

The FTIR spectra of all the capsules are presented in Fig. 4. The vibrations associated with the symmetric C–O–C bond of fatty acid ester were observed in all capsules at  $1160\text{ cm}^{-1}$  indicating the presence of essential oil.<sup>44</sup> The capsules with oregano and mustard essential oils exhibited lower intensity than the ones containing lemon and grapefruit essential oils. This is probably due to the higher encapsulation efficiency in the case of the former, which enabled a higher proportion of essential oils encapsulated inside the complex coacervates. The capsules containing lemon and grapefruit essential oils also exhibited higher absorption at  $3400\text{ cm}^{-1}$  which corresponded to stretching vibrations of –OH. The increase of intensity at  $3400\text{ cm}^{-1}$  could be attributed to the increased exposure to essential oil as the hydroxyl groups of phenolic compounds in essential oil could enhance the intensity. A previous study also reported that the presence of phenolic compounds enhanced the absorption of liposome at  $3400\text{ cm}^{-1}$  due to the presence of hydroxyl groups.<sup>45</sup> On the other hand, the constituents of essential oil that covered the surface of capsules could interact with complex coacervates through hydrogen bonds and then led to the increase of absorption at  $3400\text{ cm}^{-1}$ . The interaction



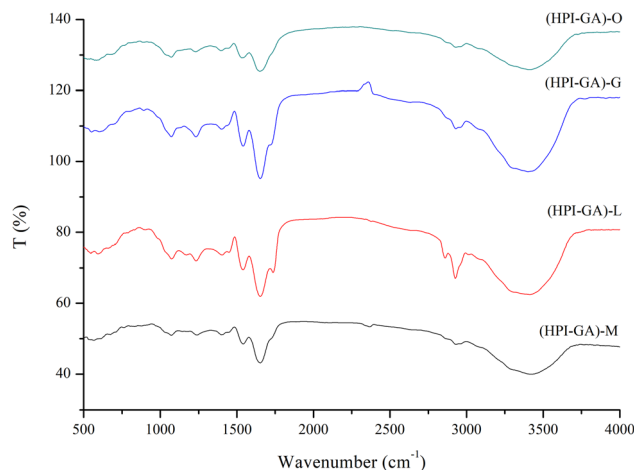


**Fig. 4** FTIR spectra of essential oils encapsulated in hemp protein isolate (HPI)–gum Arabic (GA) complex coacervates. (HPI–GA): HPI–GA complex coacervate; (HPI–GA)–M: capsules of mustard (M) essential oil in (HPI–GA) complex coacervates; (HPI–GA)–L: capsules of lemon (L) essential oil in (HPI–GA) complex coacervates; (HPI–GA)–G: capsules of grapefruit (G) essential oil in (HPI–GA) complex coacervates; (HPI–GA)–O: capsules of oregano (O) essential oil in (HPI–GA) complex coacervates.

between the constituents of essential oil and complex coacervate could also be indicated by the change of absorption at  $1600\text{ cm}^{-1}$ . Here, the capsules containing lemon and grapefruit essential oils also exhibited higher absorption due to the increased hydrophobic or electrostatic interaction.<sup>43,46</sup> This result is consistent with the observation in the particle size and microstructure. The microcapsules of lemon and grapefruit essential oils showed aggregation in the microstructure and larger particle size. The microcapsules of oregano essential oil and mustard essential oil showed relatively less aggregation.

#### Effect of essential oils on the thermal properties of capsules

The mass loss vs. temperature (TG) and its derivative (DTG) curves of the capsules are presented in Fig. 5A and B. Three distinct stages of mass loss were observed in each microcapsule (DTG curve). The first stage observed below  $100\text{ }^{\circ}\text{C}$  and the final stage observed from  $250$  to  $400\text{ }^{\circ}\text{C}$  were attributed to the loss of water and decomposition of complex coacervates, respectively.<sup>47,48</sup> The second stage observed from  $100$  to  $250\text{ }^{\circ}\text{C}$  was attributed to the volatilization of essential oil from capsules.<sup>9,49,50</sup> It can be observed that the loss of essential oil was also dependent on encapsulation efficiency. An extra derivative peak was observed in lemon essential oil capsules at lower temperature ( $131.5\text{ }^{\circ}\text{C}$ ), which could be attributed to the volatilization of essential oil on the surface of capsules due to its lower encapsulation efficiency. For the oregano essential oil capsules, an extra derivative peak was observed at much higher temperature ( $237.3\text{ }^{\circ}\text{C}$ ) which could be attributed to the volatilization of essential oil deeply buried inside the capsules due to the higher encapsulation efficiency in these capsules. This result was consistent with DSC data (Fig. 5C) that the endothermic peak shifted to higher temperature in capsules loaded

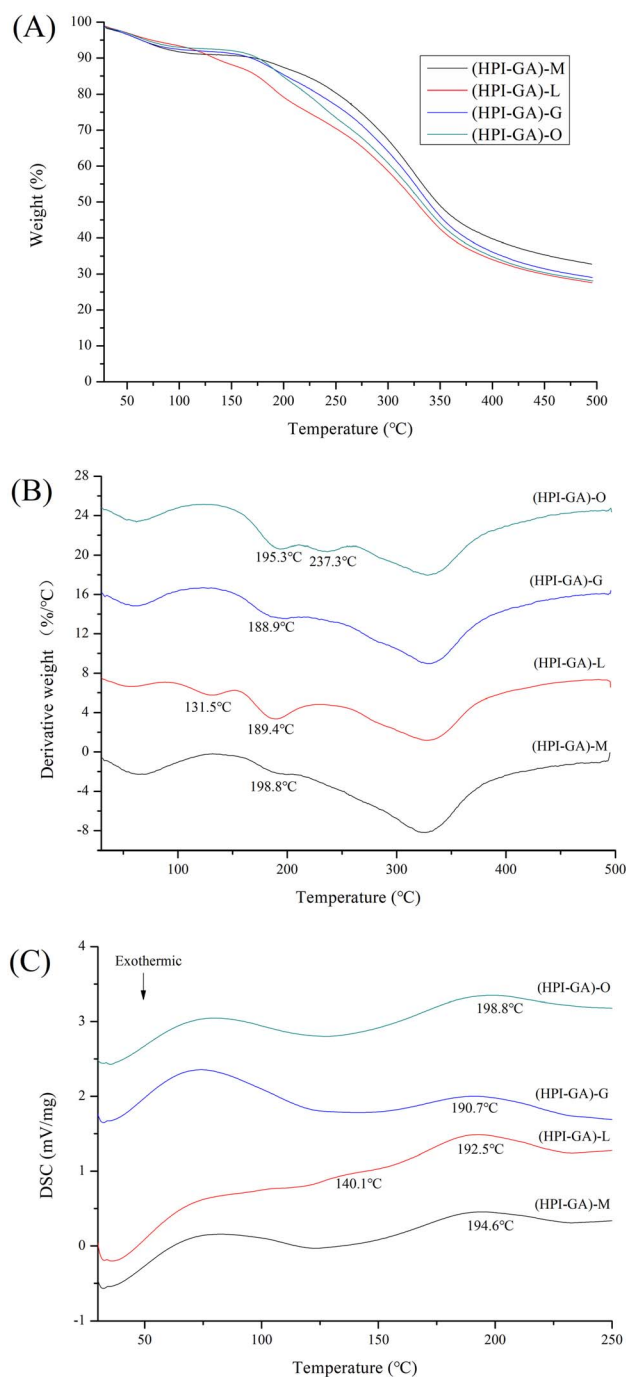


**Fig. 5** Thermogravimetry (A), derivative thermogravimetry (B) and differential scanning calorimetry (C) curves of essential oils encapsulated in hemp protein isolate (HPI)–gum Arabic (GA) complex coacervates. (HPI–GA): HPI–GA complex coacervates; (HPI–GA)–M: capsules of mustard (M) essential oil in (HPI–GA) complex coacervates; (HPI–GA)–L: capsules of lemon (L) essential oil in (HPI–GA) complex coacervates; (HPI–GA)–G: capsules of grapefruit (G) essential oil in (HPI–GA) complex coacervates; (HPI–GA)–O: capsules of oregano (O) essential oil in (HPI–GA) complex coacervates.

with oregano essential oil and an extra endothermic peak appeared at lower temperature in capsules loaded with lemon essential oil.



### Effect of essential oils on the microstructure of capsules

All of the capsules exhibited a three-dimensional network and sponge-like structure (Fig. 6). A similar microstructure was also observed in milk protein/carboxymethyl cellulose complex coacervate-based capsules loaded with  $\beta$ -pinene.<sup>51</sup> The micrographs showed that the microstructure of capsules was affected by the nature of essential oil. The oregano essential oil capsules had no obvious porosity. This result indicated that most of the oregano essential oil was entrapped inside the continuous mass of the complex coacervates. This observation corroborated with the higher encapsulation efficiency and better dispersion of these capsules in the aqueous phase. A more pronounced porous structure was observed in capsules with lower encapsulation efficiency which could explain why these microcapsules had higher surface oil. The porous structure might also lead to the exposure of active groups (*e.g.*, hydrophobic groups) which could facilitate the aggregation among capsules.

### Effect of essential oils on their controlled release

The type of essential oil significantly affected its release from capsules (Fig. 7). The release of oregano essential oil from capsules was the slowest throughout the release process, which could be attributed to a less porous structure than that of other capsules as discussed in the preceding section. Previous studies

also reported that polymers with more ordered structures reduced the release of essential oil and the polymers which could give rise to more porous structures could increase the release of essential oil.<sup>8,41</sup> The release of essential oil from each capsule was fitted well with the Weibull model with an  $R^2$  value greater than 0.95 (Table 2). The parameter  $b$  was higher than 1 for all capsules indicating that the release of essential oil from those capsules followed a complex release mechanism (combination of diffusion and swelling).<sup>52</sup> For the capsules loaded with oregano essential oil, the  $b$  value was much higher than others, indicating that release of essential oil from these capsules mainly followed matrix corrosion. This result further confirmed that capsules loaded with oregano essential oil had a more compact structure (determined through SEM) and the essential oil could be completely released only when the complex coacervate shell was ruptured. In addition, this compact structure also led to a high encapsulation efficiency in microcapsules, better dispersion in water, and better thermal stability.

### Effect of essential oils on the antioxidant properties of capsules

Essential oils possess antioxidant activity due to the presence of phenolic compounds and other secondary metabolites which can inhibit the oxidative process through mechanisms including hydrogen atom transfer, electron transfer, and the

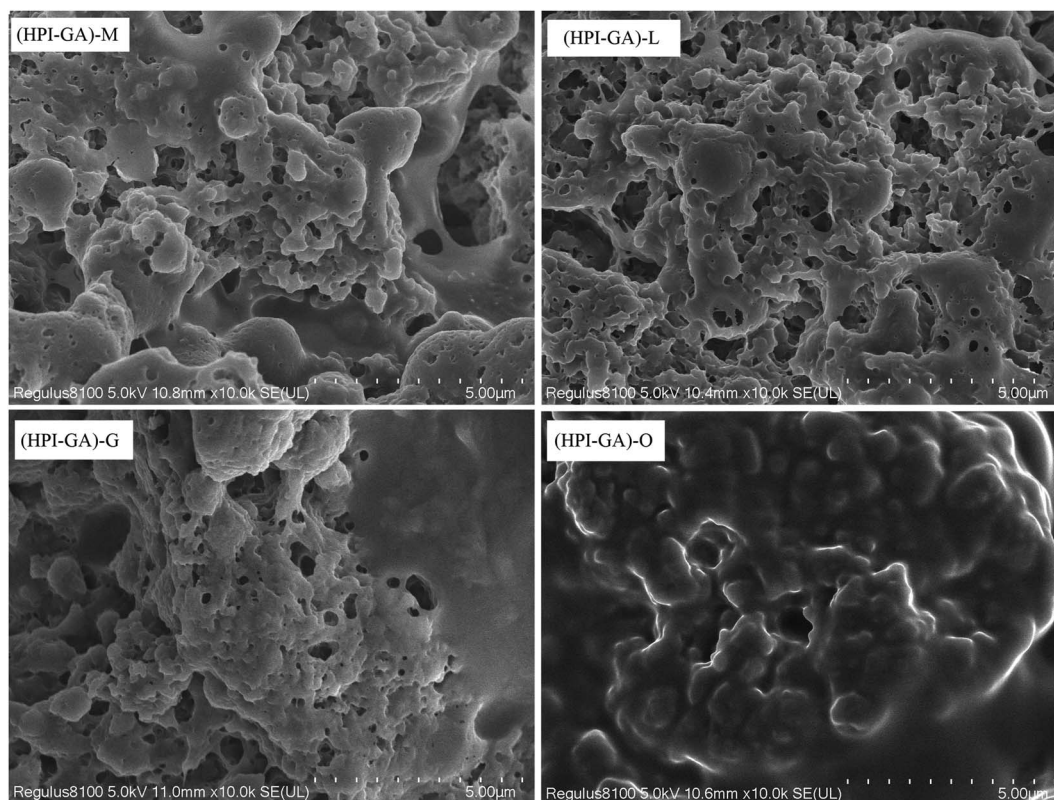


Fig. 6 Microstructure of essential oils encapsulated in hemp protein isolate (HPI)–gum Arabic (GA) complex coacervates. (HPI–GA): HPI–GA complex coacervates; (HPI–GA)–M: capsules of mustard (M) essential oil in (HPI–GA) complex coacervates; (HPI–GA)–L: capsules of lemon (L) essential oil in (HPI–GA) complex coacervates; (HPI–GA)–G: capsules of grapefruit (G) essential oil in (HPI–GA) complex coacervates; (HPI–GA)–O: capsules of oregano (O) essential oil in (HPI–GA) complex coacervates.





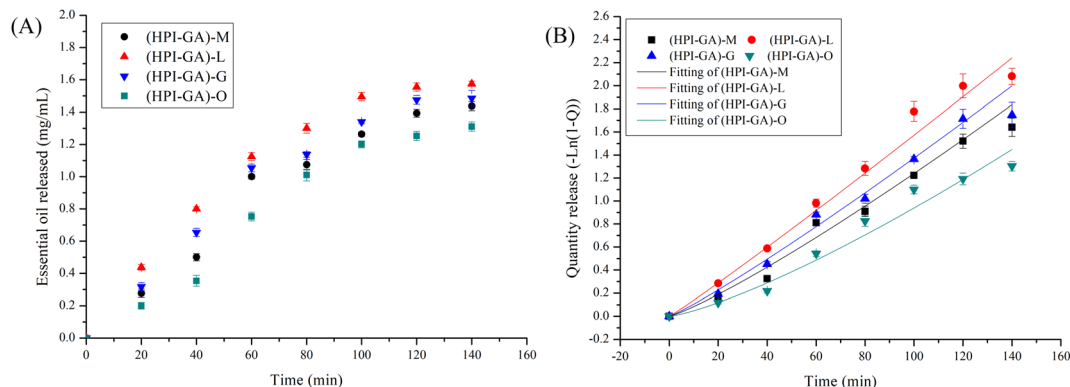


Fig. 7 Kinetics release of essential oils from hemp protein isolate (HPI)-gum Arabic (GA) complex coacervates. (HPI-GA): HPI-GA complex coacervate; (HPI-GA)-M: capsules of mustard (M) essential oil in (HPI-GA) complex coacervates; (HPI-GA)-L: capsules of lemon (L) essential oil in (HPI-GA) complex coacervates; (HPI-GA)-G: capsules of grapefruit (G) essential oil in (HPI-GA) complex coacervates; (HPI-GA)-O: capsules of oregano (O) essential oil in (HPI-GA) complex coacervates.

Table 2 Kinetics parameters of the Weibull model fitted to release data (Fig. 7)<sup>a</sup>

Sample	$R^2$	$a$	$b$
(HPI-GA)-M	$0.95 \pm 0.00$	$0.006 \pm 0.002$	$1.17 \pm 0.04$
(HPI-GA)-L	$0.99 \pm 0.00$	$0.012 \pm 0.002$	$1.05 \pm 0.03$
(HPI-GA)-G	$0.98 \pm 0.01$	$0.008 \pm 0.003$	$1.12 \pm 0.05$
(HPI-GA)-O	$0.96 \pm 0.01$	$0.002 \pm 0.001$	$1.29 \pm 0.04$

<sup>a</sup> (HPI-GA)-M: capsules of mustard (M) essential oil in (HPI-GA) complex coacervates; (HPI-GA)-L: capsules of lemon (L) essential oil in (HPI-GA) complex coacervates; (HPI-GA)-G: capsules of grapefruit (G) essential oil in (HPI-GA) complex coacervates; (HPI-GA)-O: capsules of oregano (O) essential oil in (HPI-GA) complex coacervates.

ability to chelate transition metals.<sup>53,54</sup> In general, the antioxidant activity of essential oil is affected by chemical composition, ease of volatilization, type of free radicals and the interactions between the essential oil and polymeric matrix.<sup>55</sup> As shown in Fig. 8, all capsules exhibited radical scavenging activity among which capsules loaded with oregano essential oil showed the highest antioxidant activity. This could be attributed to the better dispersion ability of capsules containing oregano essential oil and also its better protection (due to higher encapsulation efficiency) from oxidation before application. Thus, the encapsulated oregano essential oil was able to enhance the interaction between essential oil and free radicals. A previous study also reported that the interaction of polyphenols and protein in an encapsulation matrix could enhance the antioxidant activity.<sup>56</sup> The capsules loaded with mustard essential oil exhibited higher antioxidant activity than those loaded with lemon and grapefruit essential oils, which could also be attributed to its higher encapsulation efficiency. The antioxidant activity of capsules loaded with lemon essential oil is better than those loaded with grapefruit essential oil, even though the encapsulation efficiency of lemon essential oil was lower than that of grapefruit essential oil. This could be attributed to the higher content of limonene in lemon essential oil.

### Effect of essential oils on the antimicrobial properties of capsules

Essential oils impart antimicrobial function by increasing cell membrane permeability due to the lipophilic nature of essential oil.<sup>57</sup> Therefore, an essential oil can exhibit better antibacterial activity when it is in sufficient contact with microbial cells. As shown in Fig. 9, the paper loaded with chloramphenicol, which was a positive control, exhibited a visually clear inhibition zone. There was no inhibition zone for *Escherichia coli* and *Bacillus subtilis* on the paper loaded with free essential oil from lemon and grapefruit (Fig. 9). The paper loaded with mustard essential oil also did not show an inhibition zone for *Escherichia coli*. However, all the papers

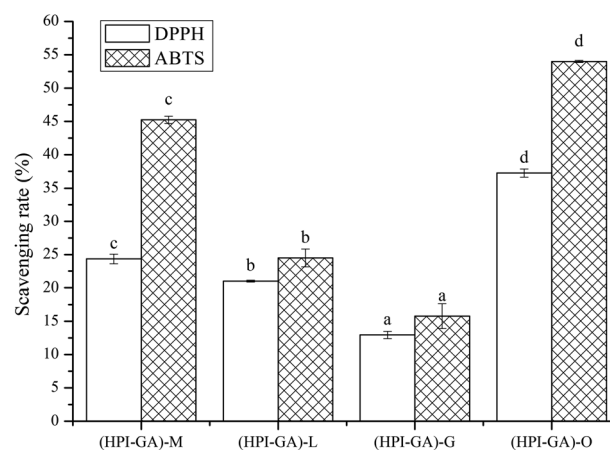
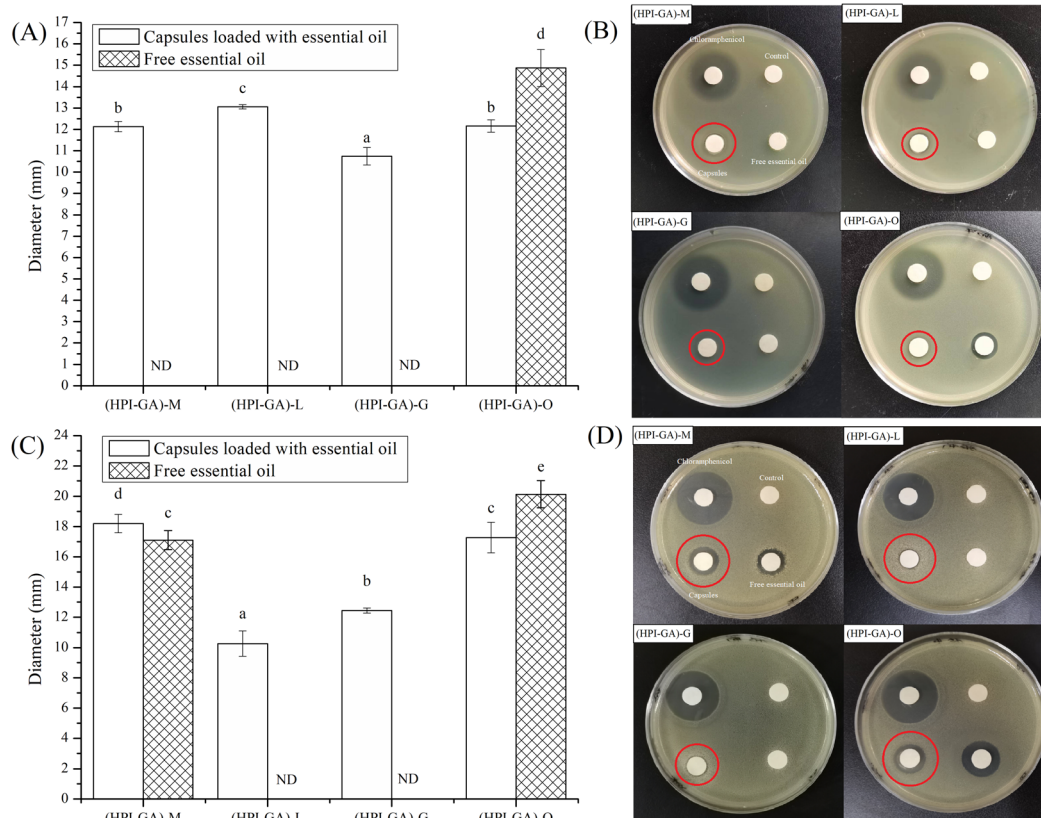


Fig. 8 Antioxidant activity of essential oils encapsulated in hemp protein isolate (HPI)-gum Arabic (GA) complex coacervates. (HPI-GA): HPI-GA complex coacervate; (HPI-GA)-M: capsules of mustard (M) essential oil in (HPI-GA) complex coacervates; (HPI-GA)-L: capsules of lemon (L) essential oil in (HPI-GA) complex coacervates; (HPI-GA)-G: capsules of grapefruit (G) essential oil in (HPI-GA) complex coacervates; (HPI-GA)-O: capsules of oregano (O) essential oil in (HPI-GA) complex coacervates. Superscripts (a-d) with the different letters in the same pattern were significantly different ( $p < 0.05$ ).







**Fig. 9** Antibacterial activity of essential oils encapsulated in hemp protein isolate (HPI)–gum Arabic (GA) complex coacervates. (HPI–GA): HPI–GA complex coacervates; (HPI–GA)–M: capsules of mustard (M) essential oil in (HPI–GA) complex coacervates; (HPI–GA)–L: capsules of lemon (L) essential oil in (HPI–GA) complex coacervates; (HPI–GA)–G: capsules of grapefruit (G) essential oil in (HPI–GA) complex coacervates; (HPI–GA)–O: capsules of oregano (O) essential oil in (HPI–GA) complex coacervates. ND: antibacterial activity was not detected. (A) and (B) represent inhibition to *Escherichia coli*. (C) and (D) represent inhibition to *Bacillus subtilis*. Superscripts (a–d) with the different letters were significantly different ( $p < 0.05$ ).

loaded with capsules exhibited antibacterial activity (Fig. 9). This could be attributed to the fact that encapsulation was able to improve the compatibility between essential oil and culture medium, so as to exert the antibacterial activity of essential oil. Encapsulation could also release the essential oil in a controlled fashion which is conducive to achieving the antibacterial effect. Interestingly, the free oregano essential oil exhibited a bigger inhibition zone than its capsule. This might be due to the fact that antibacterial substances contained in oregano essential oil were less volatile by nature and the residue on the paper could still impart antimicrobial function. Furthermore, there was no obvious correlation between antibacterial activity and encapsulation efficiency, which is probably due to the different sensitivity of microorganisms to essential oil components.

## Conclusion

The outcomes of this study provide insights into the development of HPI–GA coacervates as wall materials for encapsulation of essential oils. It was found that the type of essential oil affected the encapsulation efficiency as well as the release pattern and physical, structural, antioxidant and antibacterial

properties of the resulting capsules. The capsules loaded with oregano essential oil had a more compact structure and achieved the highest encapsulation efficiency and enabled better dispersion in the aqueous phase. The capsules containing essential oregano oil also had better thermal stability and lower release rate. The capsules loaded with oregano essential oil also exhibited higher radical scavenging activity. The capsules containing all of the tested essential oils (oregano, mustard, lemon and grapefruit essential oils) exhibited a higher inhibitory effect against *Escherichia coli* and *Bacillus subtilis* than the corresponding free essential oil. The release of essential oil from all capsules fitted well with the Weibull model and followed a complex release mechanism. These microcapsules can be used as preservatives to extend the shelf life of food products. Their increased application as preservatives is aided by their good solubility, ease of incorporation into food systems and demonstratively high antioxidant and antibacterial activities.

## Data availability statement

The data that support the findings of this study can be made available upon request.



## Author contributions

Xinye Liu: conceptualization, methodology and data curation; Feng Xue: project administration, formal analysis, investigation and writing original draft; Benu Adhikari: supervision, conceptualization, methodology, review and editing.

## Conflicts of interest

The authors have no conflict of interest to declare.

## Acknowledgements

This work was supported by The Open Project of Chinese Materia Medica First-Class Discipline of Nanjing University of Chinese Medicine (2020YLXK021) and the Natural Science Foundation of the Jiangsu Higher Education Institutions of China (20KJB550014).

## References

- 1 S. Burt, *Int. J. Food Microbiol.*, 2004, **94**, 223–253.
- 2 F. Bakkali, S. Averbeck, D. Averbeck and M. Idaomar, *Food Chem. Toxicol.*, 2008, **46**, 446–475.
- 3 N. Mohammadi and N. Ostovar, *Food Chem. Adv.*, 2022, **1**, 100066.
- 4 A. Coimbra, S. Ferreira and A. P. Duarte, *Food Chem.*, 2022, **393**, 133370.
- 5 E. Padilla-Camberos, I. M. Sanchez-Hernandez, O. R. Torres-Gonzalez, M. d. R. Gallegos-Ortiz, A. L. Méndez-Mona, P. Baez-Moratilla and J. M. Flores-Fernandez, *Saudi J. Biol. Sci.*, 2022, **29**, 3830–3837.
- 6 A. M. Bakry, S. Abbas, B. Ali, H. Majeed, M. Y. Abouelwafa, A. Mousa and L. Liang, *Compr. Rev. Food Sci. Food Saf.*, 2016, **15**, 143–182.
- 7 D. R. Reis, A. Ambrosi and M. D. Luccio, *Future Foods*, 2022, **5**, 100126.
- 8 F. Xue, Y. Gu, Y. Wang, C. Li and B. Adhikari, *Food Hydrocolloids*, 2019, **96**, 178–189.
- 9 X. Liu, F. Xue, C. Li and B. Adhikari, *Int. J. Biol. Macromol.*, 2022, **202**, 26–36.
- 10 A. Sedaghat Doost, M. Nikbakht Nasrabadi, J. Wu, Q. A'Yun and P. Van der Meer, *Trends Food Sci. Technol.*, 2019, **91**, 1–11.
- 11 M. A. Augustin, L. Sanguansri and O. Bode, *J. Food Sci.*, 2006, **71**, E25–E32.
- 12 Z. Zhang, B. Wang and B. Adhikari, *Future Foods*, 2022, **6**, 100193.
- 13 Z. Zhang, G. Holden, B. Wang and B. Adhikari, *Food Chem.*, 2023, **406**, 134931.
- 14 T. Li, L. Niu, X. Li, F. Wang, Y. Huang and Y. Liu, *Food Chem.*, 2022, **395**, 133612.
- 15 Y. Lv, F. Yang, X. Li, X. Zhang and S. Abbas, *Food Hydrocolloids*, 2014, **35**, 305–314.
- 16 R. Hernández-Nava, A. López-Malo, E. Palou, N. Ramírez-Corona and M. T. Jiménez-Munigua, *Food Hydrocolloids*, 2020, **109**, 106077.
- 17 L. P. Heckert Bastos, J. Vicente, C. H. Corrêa dos Santos, M. Geraldo de Carvalho and E. E. Garcia-Rojas, *Food Hydrocolloids*, 2020, **102**, 105605.
- 18 T. A. Comunian, A. Archut, L. G. Gomez-Mascaraque, A. Brodkorb and S. Drusch, *Carbohydr. Polym.*, 2022, **295**, 119851.
- 19 R. Shaddel, J. Hesari, S. Azadmard-Damirchi, H. Hamishehkar, B. Fathi-Achachlouei and Q. Huang, *Int. J. Biol. Macromol.*, 2018, **107**, 1800–1810.
- 20 W. Luo, H. Huang, Y. Zhang, F. Wang, J. Yu, Y. Liu and X. Li, *LWT-Food Sci. Technol.*, 2021, **150**, 112084.
- 21 S. Sharifi, M. Rezazad-Bari, M. Alizadeh, H. Almasi and S. Amiri, *Food Hydrocolloids*, 2021, **113**, 106496.
- 22 X. Jun-xia, Y. Hai-yan and Y. Jian, *Food Chem.*, 2011, **125**, 1267–1272.
- 23 S. F. Mirpoor, C. V. L. Giosafatto, R. Di Girolamo, M. Famiglietti and R. Porta, *Food Packag. Shelf Life*, 2022, **31**, 100779.
- 24 X. Liu, F. Xue and B. Adhikari, *Food Hydrocolloids*, 2023, **137**, 108352.
- 25 F. Plati, C. Ritzoulis, E. Pavlidou and A. Paraskevopoulou, *Int. J. Biol. Macromol.*, 2021, **182**, 144–153.
- 26 X. Liu, M. Wang, F. Xue and B. Adhikari, *Future Foods*, 2022, **6**, 100176.
- 27 S. Liu, N. H. Low and M. T. Nickerson, *J. Am. Oil Chem. Soc.*, 2010, **87**, 809–815.
- 28 D. Eratte, B. Wang, K. Dowling, C. J. Barrow and B. P. Adhikari, *Food Funct.*, 2014, **5**, 2743–2750.
- 29 J. K. Alarcón-Moyano, R. O. Bustos, M. L. Herrera and S. B. Matiacevich, *J. Food Sci. Technol.*, 2017, **54**, 2878–2889.
- 30 V. Papadopoulou, K. Kosmidis, M. Vlachou and P. Macheras, *Int. J. Pharm.*, 2006, **309**, 44–50.
- 31 S.-C. Liu, J.-T. Lin, C.-K. Wang, H.-Y. Chen and D.-J. Yang, *Food Chem.*, 2009, **114**, 577–581.
- 32 Y.-L. Chew, J.-K. Goh and Y.-Y. Lim, *Food Chem.*, 2009, **116**, 13–18.
- 33 B. Li, J. F. Kennedy, J. L. Peng, X. Yie and B. J. Xie, *Carbohydr. Polym.*, 2006, **65**, 488–494.
- 34 L. P. H. Bastos, C. H. C. dos Santos, M. G. de Carvalho and E. E. Garcia-Rojas, *Food Chem.*, 2020, **316**, 126345.
- 35 E. F. de Matos, B. S. Scopel and A. Dettmer, *J. Environ. Chem. Eng.*, 2018, **6**, 1989–1994.
- 36 A. S. Prata and C. R. F. Grosso, *J. Am. Oil Chem. Soc.*, 2015, **92**, 1063–1072.
- 37 Y. Wang, R. Lin, Z. Song, S. Zhang, X. Zhao, J. Jiang and Y. Liu, *Food Hydrocolloids*, 2022, **125**, 107385.
- 38 M. Tabatabaei, A. Rajaei, E. Hosseini, M. Aghbashlo, V. K. Gupta and S. S. Lam, *Carbohydr. Polym.*, 2022, **291**, 119566.
- 39 C. Peng, S.-Q. Zhao, J. Zhang, G.-Y. Huang, L.-Y. Chen and F.-Y. Zhao, *Food Chem.*, 2014, **165**, 560–568.
- 40 R. Duan and M. Qi, *J. Chromatogr. A*, 2021, **1658**, 462611.
- 41 C. Li, J. Pei, X. Xiong and F. Xue, *Coatings*, 2020, **10**, 784.
- 42 F. Plati and A. Paraskevopoulou, *Food Hydrocolloids*, 2023, **136**, 108284.
- 43 Q. Guo, S. Li, G. Du, H. Chen, X. Yan, S. Chang, T. Yue and Y. Yuan, *LWT-Food Sci. Technol.*, 2022, **165**, 113683.



- 44 R. Jamwal, Amit, S. Kumari, S. Sharma, S. Kelly, A. Cannavan and D. K. Singh, *Vib. Spectrosc.*, 2021, **113**, 103222.
- 45 N. A. Ramli, N. Ali, S. Hamzah and N. I. Yatim, *Heliyon*, 2021, **7**, e06649.
- 46 L. Mei, Q. Ji, Z. Jin, T. Guo, K. Yu, W. Ding, C. Liu, Y. Wu and N. Zhang, *LWT-Food Sci. Technol.*, 2022, **163**, 113550.
- 47 L. Zhang, Z. Zhang, Y. Chen, X. Ma and M. Xia, *Food Chem.*, 2021, **338**, 128013.
- 48 C. Li, P. Jiliu, S. Zhu, Y. Song, X. Xiong and F. Xue, *Coatings*, 2020, **10**, 1193.
- 49 A. E. Asbahani, K. Miladi, W. Badri, M. Sala, E. H. A. Addi, H. Casabianca, A. E. Mousadik, D. Hartmann, A. Jilale, F. N. R. Renaud and A. Elaissari, *Int. J. Pharm.*, 2015, **483**, 220–243.
- 50 F. M. Bezerra, O. G. Carmona, C. G. Carmona, M. J. Lis and F. F. de Moraes, *Cellulose*, 2016, **23**, 1459–1470.
- 51 T. Koupantsis, E. Pavlidou and A. Paraskevopoulou, *Food Hydrocolloids*, 2016, **57**, 62–71.
- 52 J. Siepmann and N. A. Peppas, *Adv. Drug Delivery Rev.*, 2012, **64**, 163–174.
- 53 D. Granato, F. Shahidi, R. Wrolstad, P. Kilmartin, L. D. Melton, F. J. Hidalgo, K. Miyashita, J. v. Camp, C. Alasalvar, A. B. Ismail, S. Elmore, G. G. Birch, D. Charalampopoulos, S. B. Astley, R. Pegg, P. Zhou and P. Finglas, *Food Chem.*, 2018, **264**, 471–475.
- 54 S. Bhavaniramy, S. Vishnupriya, M. S. Al-Aboody, R. Vijayakumar and D. Baskaran, *Grain Oil Sci. Technol.*, 2019, **2**, 49–55.
- 55 A. Acevedo-Fani, L. Salvia-Trujillo, M. A. Rojas-Graü and O. Martín-Belloso, *Food Hydrocolloids*, 2015, **47**, 168–177.
- 56 Y. Guo, Y.-h. Bao, K.-f. Sun, C. Chang and W.-f. Liu, *Food Hydrocolloids*, 2021, **112**, 106293.
- 57 B. D. da Silva, D. K. A. do Rosário, D. A. Weitz and C. A. Conte-Junior, *Trends Food Sci. Technol.*, 2022, **121**, 1–13.

